

Received September 8, 2021, accepted September 20, 2021, date of publication September 22, 2021, date of current version September 29, 2021.

Digital Object Identifier 10.1109/ACCESS.2021.3114598

# Optimal Sizing of CPP-GMR Read Sensors for Magnetic Recording Densities of 1–4 Tb/in<sup>2</sup>

PIRAT KHUNKITTI<sup>1</sup>, (Member, IEEE), KOTCHAKORN PITUSO<sup>2</sup>, NUTTAPON CHAIDUANGSRI<sup>2</sup>, AND APIRAT SIRITARATIWAT<sup>1</sup>

<sup>1</sup>KKU-Seagate Cooperation Research Laboratory, Department of Electrical Engineering, Faculty of Engineering, Khon Kaen University, Khon Kaen 40002, Thailand

<sup>2</sup>Seagate Technology (Thailand) Ltd., Samut Prakarn 10270, Thailand

Corresponding author: Pirat Khunkitti (piratk@kku.ac.th)

This work was financially supported by Office of the Permanent Secretary, Ministry of Higher Education, Science, Research and Innovation, under Grant RGNS 63-058.

**ABSTRACT** Several studies have confirmed that current-perpendicular-to-the-plane giant magnetoresistance (CPP-GMR) technology is appropriate for next-generation read sensors for ultrahigh areal densities (ADs) of data storage applications. Since the physical dimension of the read sensor is a crucial factor for developing the reader to overcome its limitations, this paper proposes an optimal sizing prediction of the CPP-GMR read heads for ADs of 1–4 Tb/in<sup>2</sup>. Micromagnetic modelling was performed in the simulations. The appropriate length of the stripe height (SH) and the read width (RW) of the readers was estimated based on a consideration of sensor outputs including the readback signal, asymmetry parameter, dibit response and power spectral density (PSD) profile. It was found that a variation of SH and RW lengths had an influential impact on the readback signal waveform. Those affectations were further characterized through the echoes of dibit response showing that shortening the SH length or increasing the RW length could improve the resolution and reduce the distortion occurring in the readback signal. Moreover, the PSD profile indicated that the reader operation became more stable at shorter SH lengths or longer RW lengths. The head response spectrum was also examined. In addition, the magnitude of the bias current was studied in relation to the head response. Lastly, the optimal physical dimension (SH × RW) of the CPP-GMR readers for ADs of 1–4 Tb/in<sup>2</sup> was predicted to be (40 × 48) nm, (28 × 29) nm, (25 × 26) nm and (19 × 20) nm, respectively. The results can be utilized to design the CPP-GMR sensors at ultrahigh magnetic recording capacities.

**INDEX TERMS** Magnetic recording, magnetic read heads, current perpendicular-to-the-plane giant magnetoresistance, Heusler alloys.

## I. INTRODUCTION

As the areal density (AD) of the hard disk drive (HDD) is expected to reach 10 Tb/in<sup>2</sup> in the coming decade, challenges in developing the magnetic recording heads to deal with a shrinking of media bit size have been extensively researched [1]–[3]. The current-perpendicular-to-the-plane giant magnetoresistance (CPP-GMR) sensors have been promising candidates to overcome the limitations to reach ultrahigh storage capacities, due mainly to their extremely small resistance-area and their high rate of data transfer [4]–[6]. Also, a shorter read gap and better electrode contact for the CPP-GMR sensors can be better achieved

compared to the magnetic tunnel junction (MTJ) currently used in the hard disk drive [4], [7]. However, the main drawback of the GMR technologies is their small magnetoresistance (MR) ratio compared to the tunneling magnetoresistive devices [8], [9]. Therefore, the ferromagnetic Heusler alloys have been extensively proposed as potential materials to compensate for this weakness of the CPP-GMR efficiently [10]–[13]. The outstanding property of these alloys is their extremely high spin polarization with high robustness, which can greatly improve the MR ratio of the CPP-GMR devices, as widely reported in several studies [14]–[17].

At higher recording densities, in which the magnetic bit size needs to be rapidly shrunk, the physical dimension of the reader has to be extremely downsized to maintain a sufficient resolution as well as to avoid the unwanted side reading

The associate editor coordinating the review of this manuscript and approving it for publication was Philip Pong<sup>1</sup>.

from adjacent tracks [18]. Shrinking of the CPP-GMR readers normally degrades their signal-to-noise ratio (SNR); moreover, the heads also become more sensitive to noise, e.g. the thermally activated magnetization fluctuation noise (mag-noise) and the spin transfer torque induced noise [19]–[23]. Therefore, a suitable physical dimension of the CPP-GMR sensors, especially at higher ADs, becomes a crucial factor since it significantly impacts the read head performance. A decade ago, the dimension of a CPP-GMR read head at high ADs was forecasted [2], [18]. However, we noticed that a more precise prediction of reader dimension can be made, since a few essential factors such as the mag-noise, the spin-transfer induced instabilities, magnetic media materials and the use of novel materials, e.g. Heusler alloys have not been included in the literature yet.

Then, we proposed a sizing prediction of the CPP-GMR read heads by evaluating a suitable length of the stripe height (SH) and the reader width (RW) of the heads for ADs of 1-4 Tb/in<sup>2</sup>. The CPP-GMR heads based on Co<sub>2</sub>(Mn<sub>0.6</sub>Fe<sub>0.4</sub>)Ge (CMFG) Heusler alloy were focused on. The performance indicators of the read sensors, including the readback signal, asymmetry parameter, dibit response and power spectral density (PSD) profile were analyzed and discussed. The micromagnetic simulations were based on the finite element method using M3 code [24]. The results can be utilized to design the CPP-GMR sensors at the ultrahigh capacities of magnetic recording applications.

## II. MODEL AND CALCULATION

### A. MODELLING OF THE CPP-GMR READ SENSORS

The sensing layers model of a CPP-GMR reader for AD of 1 Tb/in<sup>2</sup> while operating is shown in Fig. 1(a). The free/non-magnetic/reference layers (thickness) were made of CMFG(5 nm)/AgSn/InZnO(2.1 nm)/CMFG(5 nm), this composition was adopted from Nakatani *et al.* [25]. The magnetization of the free layer was initialized along its easy axis (y-axis) along the RW direction; while the magnetization of the reference layer was aligned fixedly along the +x-axis due to the exchange bias effect of the anti-ferromagnetic layer. Soft magnetic shields were also included in the model with a shield-to-shield spacing previously predicted by Takagishi *et al.* [2]. During operation, the magnetization of the free layer was assumed to be ±30° tilted while receiving the magnetic stray field,  $H_{stray}$ , from the medium. The hard-bias field,  $H_B$ , was applied to the read head with a uniform pattern for biasing the magnetization of the free layer. Accordingly, the magnitude of  $H_B$  could vary depending on the reader dimension. At ADs greater than 1 Tb/in<sup>2</sup>, many studies have claimed that the FePt is the most attractive material to overcome the thermal stability limitation at those capacities [26]–[28]. In this work, the medium was assumed to be a perpendicular media based on a 10 nm thickness of the FePt hard layer. The bit length and track width of the FePt media for ADs of 1-4 Tb/in<sup>2</sup> were based on the prediction previously given by Han *et al.* [18]. Figure 1(b) shows the

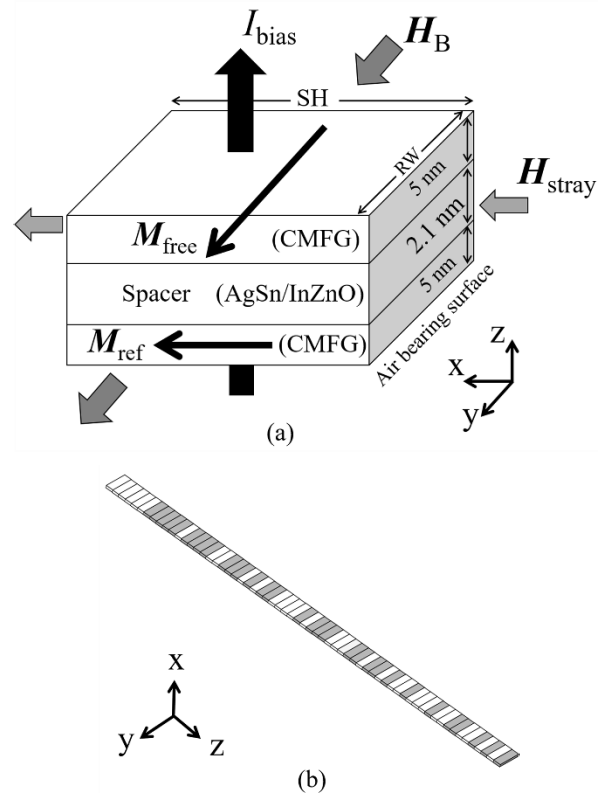


FIGURE 1. (a) Modeling of CPP-GMR sensor for AD of 1 Tb/in<sup>2</sup> and (b) randomly generated magnetic bits.

63 pseudorandom bit sequence (PRBS) along a cross-track direction. A magnetic bit was assumed to have a bit aspect ratio of 4 since this value can be possible at higher areal densities. The PRBS generator polynomial used in this work was  $x^6 + x^5 + 1$  [29]. The recorded bits were assumed to have no writing error or intertrack interference, therefore the transition noise was neglected in the calculations. The direction of  $H_{stray}$  was along the x-axis which is perpendicular to the air bearing surface. The gray and white filled bits indicate the direction of  $H_{stray}$  along the +x and -x axis, respectively. The magnitude of  $H_{stray}$  generated by the medium can be known by an analytical calculation given in [30]. The head was assumed to be operated at 1 GHz for all ADs, since this value is sufficient for practical applications.

The material properties of CMFG Heusler alloy are indicated as follows: saturation magnetization,  $M_s$ , of  $10 \times 10^5$  A/m, anisotropy constant of  $8 \times 10^3$  J/m<sup>3</sup>, spin polarization factor,  $p$ , of 0.76, Gilbert damping parameter,  $\alpha$ , of 0.01, and exchange stiffness constant,  $A$ , of  $2.25 \times 10^{-11}$  J/m [25]. The sensing layers have a resistance area (RA) product and MR ratio of  $0.11 \Omega\mu\text{m}^2$  and 32%, respectively. A constant bias current was applied to the head to produce the readback voltage of 1 mV for all cases. The positive current was defined as a current flowing from the reference to the free layers. The time dependence of the magnetization dynamic with the inclusion of the

spin polarized current is computed by the Landau-Lifshitz-Gilbert-Slonczewski formula, given as a summation of precession, damping and spin transfer torque (STT) terms [31]:

$$\frac{d\mathbf{M}}{dt} = -\gamma\mathbf{M} \times \mathbf{H}_{\text{eff}} - \alpha \frac{\gamma}{M_s} \mathbf{M} \times (\mathbf{M} \times \mathbf{H}_{\text{eff}}) - a_j \frac{\gamma}{M_s} \mathbf{M} \times (\mathbf{M} \times \mathbf{m}_p) \quad (1)$$

where  $\mathbf{M}$ ,  $\mathbf{H}_{\text{eff}}$ ,  $\mathbf{m}_p$  and  $\gamma$  are the magnetization, effective magnetic field, unit vector along polarization direction and gyromagnetic ratio, respectively. The  $a_j = (J\hbar g(\theta))/(2eM_s\delta)$  is a spin torque factor where  $J$  is the polarized current density,  $\hbar$  is the reduced Planck's constant,  $e$  is the electron charge value and  $\delta$  is the free layer thickness. The scalar function is given as  $g(\theta) = [-4 + (1 + p)^3(3 + \cos\theta)/4p^{3/2}]^{-1}$ , where  $\theta$  is the angle between the magnetizations of the free layer and the reference layer. A  $2.5 \times 2.5 \times 2.5$  nm<sup>3</sup> computational cell size and 0.1 ps time step were set for all cases of the simulations.

To predict the optimal sizing of the CPP-GMR read heads for ADs of 1–4 Tb/in<sup>2</sup>, an appropriate length of the SH and RW for all ADs was evaluated under the condition the system is based on the conventional reader operation, as well as conventional perpendicular media. The possible varying range of SH and RW was limited based on the condition that the magnetization of the head could be  $\pm 30^\circ$  tilt while operating. Beyond this considered range, the magnetization of the free layer was not able to be stabilized with  $\pm 30^\circ$  tilted during an operation due to an incompatibility of the hard-bias field and the anisotropy field. It was also noted that the length of SH or RW was individually adjusted for all cases of investigations, so that the length of RW was fixed during an adjustment of the SH length and vice versa.

### B. ANALYSIS OF THE READER CHARACTERISTICS

In this work, we predicted the optimal sizing of the CPP-GMR readers through the characteristics of the head response including the readback signal, asymmetry parameter, dibit response and power spectral density (PSD) profile. Typically, these factors could evidently indicate the performance of the detector scheme. To obtain the readback signal, the magnetization dynamic of the free layer was first collected. Then, the readback signal was computed by applying a Butterworth low-pass filter to the magnetization response [32]. The asymmetry of the readback signal was obtained from the difference of the positive and negative readback amplitudes divided by a summation of those amplitudes, as written in (2) [33].

$$\%Asymmetry = \frac{(V_p - V_n)}{(V_p + V_n)} \times 100 \quad (2)$$

The dibit response of the readback signal can demonstrate the channel transfer function, nonlinear behavior and distortion occurring in the waveform [34]. In this step, the time domain dibit extraction technique was performed to obtain the linear dibit response as well as the nonlinearities via

echoes around the main pulses [35]. These echoes typically occur at certain locations which can be calculated by the finite Volterra series of PRBS. The Volterra series describes that the channel output is a superposition of the linear output and nonlinear parts. With the unique ‘‘Shift-and-Add’’ property of PRBS, the main linear pulse is presented at the center of the dibit response while the other nonlinear echoes occur at certain locations depending on the PRBS length and the polynomial [29].

In general, the noise arising in the reading sensors is an important factor indicating the SNR. For the CPP-GMR sensors, the Johnson noise is extremely small compared to the MTJ, while the shot noise is nonexistence. These disturbances are therefore neglected in our evaluations. However, the mag-noise plays a crucial role in the stability of CPP-GMR sensors. The magnitude of mag-noise increases inversely with the sensor volume; accordingly, this noise needs to be of concern at higher ADs where the reader dimension becomes downscaled. For the read sensors having a CPP stack, the STT effect has been widely known as a significant factor related to the mag-noise behavior since it typically causes disturbance in the magnetization precession. Accordingly, the STT induced instability may bring about the magnetization fluctuation yielding an enlargement of mag-noise. In general, the scale of mag-noise can be evaluated through the PSD of the time-varying magnetization. To obtain the total PSD intensity, the local PSD was firstly calculated through the time dependence of the magnetization configuration,  $\mathbf{M}_{x,y,z}(r_i, t_j)$ , where  $r_i$  is the magnetization position at each varying time,  $t_j$ , given in (3) [36].

$$S_{x,y,z}(r_i, f) = \left| \sum_j \mathbf{M}_{x,y,z}(r_i, t_j) e^{i2\pi f t_j} \right|^2 \quad (3)$$

Then, the total PSD was computed by a summation of the local PSD at each particular frequency,  $S_{x,y,z}(r_i, f)$ , given as (4). An integrated PSD can be further obtained by an integral of the overall PSD.

$$\bar{S}_{x,y,z}(f) = \sum_j S_{x,y,z}(r_i, f) \quad (4)$$

## III. RESULTS AND DISCUSSION

### A. OPTIMAL SIZING OF THE CPP-GMR SENSOR FOR AD OF 1 TB/in<sup>2</sup>

We firstly evaluated the optimal sizing of the CPP-GMR reader for an AD of 1 Tb/in<sup>2</sup> based on a consideration of reader outputs including the readback signal, dibit response, asymmetry parameter and the PSD profile. At this recording density, the media bit length and track width were previously predicted to be 12.5 and 51 nm, respectively, which is related to the TPI and BPI of 500 kTPI and 2000 kBPI, respectively [18]. The reader gap was assumed to be 24.7 nm. Also, the conventional dimension of the CPP-GMR sensor can be set as the SH length of 40 nm and the RW length of 36 nm [18]. The possible range of SH variation

was 28 to 50 nm and that of RW was 18 to 48 nm. This range was limited by the condition that the readers could be operated with  $\pm 30^\circ$  tilt of the free layer magnetization while receiving the  $H_{\text{stray}}$ , so that the sensor utilization is the same for all cases. Additionally, the limitations that the RW length has to be less than the  $0.95 \times$  media track width as well as the SH should not exceed  $1.1 \times$  RW were included [37]. It was noticed that the length of RW was fixed while varying the length of SH and vice versa for all case studies.

The readback signal of the CPP-GMR sensors at various lengths of SH and RW is shown in Fig. 2(a) and 2(b), respectively. The RW was fixed to be 36 nm for the result shown in Fig. 2(a), while the SH was fixed to be 40 nm for that shown in Fig. 2(b). When varying the read head dimension, it was found that the readback signal became more distorted at longer SH lengths and shorter RW lengths. In particular, the signal was highly distorted at the RW length of 18 nm. The distortion scales of those will be evaluated through the dibit response. On the other hand, an important finding was that the readback signal became more symmetric and less distorted at shorter SH and longer RW lengths. Higher distortion of signal from the head with longer SH and shorter RW lengths can be physically explained by the behavior of the demagnetization field,  $H_{\text{demag}}$ , over the free layer region [3]. The  $H_{\text{demag}}$  is theoretically a force pulling the magnetization toward the its opposite direction, which results in fluctuating magnetization dynamic causing higher instabilities. In general, the  $H_{\text{demag}}$  is micromagnetically inhomogeneous over the free layer region. It typically has more intensity along the edge of the SH side than that of the RW side. So, the reader with longer SH and shorter RW lengths is expected to have higher instability, as well as signal distortion.

In addition, it is seen that the distortion of the readback signal occurred mostly at the positive readback signal rather than the negative voltage. This was because only the positive bias current was considered in the investigations. From the simulation model, the positive bias current resulted in current induced spin transfer, which attempted to bring about the anti-parallel state between the magnetization of free and reference layers, since the reflected electron from the reference layer (in the  $-x$  direction) flowed as an incident electron on the free layer. Then, the anti-parallel magnetization alignment of those layers was more stable than the parallel magnetization alignment. From the readback signal generation, the positive side of the waveform was generated by the  $H_{\text{stray}}$  in the  $+x$  direction in which the magnetization of the free layer was tilted antiparallel to the magnetization of the reference layer, whereas, the stray field in the  $-x$  direction yielded the parallel state of magnetization that produces the negative readback signal. Therefore, any occurrence of distortion in the readback signal can be evidently seen in the positive waveform rather than the negative waveform. However, there was no error bit detected in the investigations since the amplitude of the readback signal for all cases was in the acceptable range for the signal processing.

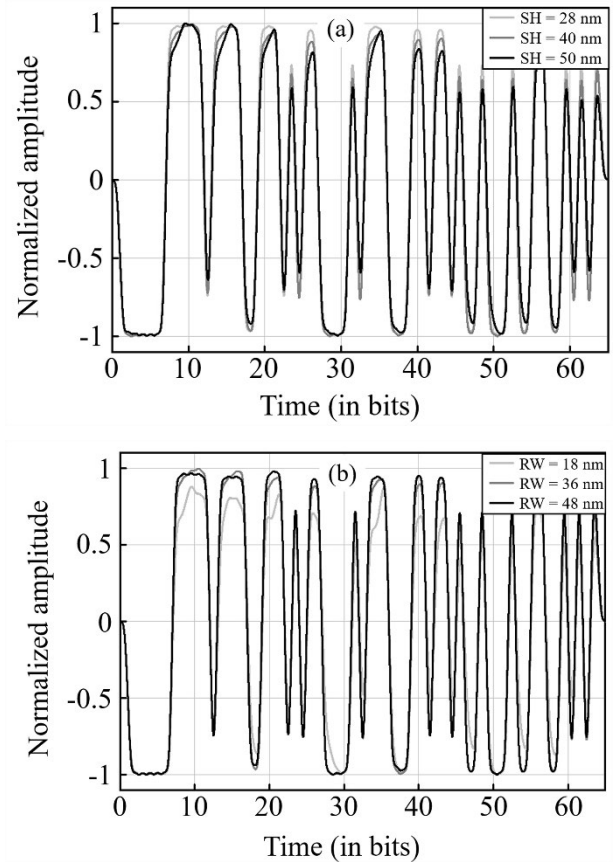


**FIGURE 2.** The readback signal of the CPP-GMR sensors for AD of 1 Tb/in<sup>2</sup> at various lengths of (a) SH and (b) RW.

To get an insight into the distortion behavior of the readback signal, the time domain dibit extraction technique was performed. Figures 3(a) and 3(b) illustrate the dibit response of the readback signal generated by the CPP-GMR sensors with different SH and RW lengths. The length of RW was fixed while varying the length of SH and vice versa. The insets indicate the magnified images of echoes. From the dibit response of 63-bit PRBS with the polynomial  $x^6 + x^5 + 1$ , the echoes  $C_1^{(2)}$ ,  $C_2^{(2)}$  and  $C_{1,2}^{(3)}$  respectively located at bit periods of 27, 22 and 8 were the main echoes indicating the non-linear distortion of the readback waveform [35]. The impacts of higher orders of echoes were dominated by these main echoes and can be ignored in the evaluations. From the dibit response, it was obviously found that the reader having the SH of 50 nm contained significantly higher echo amplitude at 8- and 22-bit periods than that of other SH lengths. The reader with the SH of 28 nm, on the other hand, indicated the smallest echoes, implying that this head may have better linearity and lower distortion than the others. Meanwhile, the sensor having the RW of 18 nm showed a larger echo at the 8-bit period and higher undershoot at 22- and 27-bit periods than the others. Remarkably, the reader with an RW length of 48 nm demonstrated a very small echo amplitude showing that this reader produced a highly stable readback waveform.



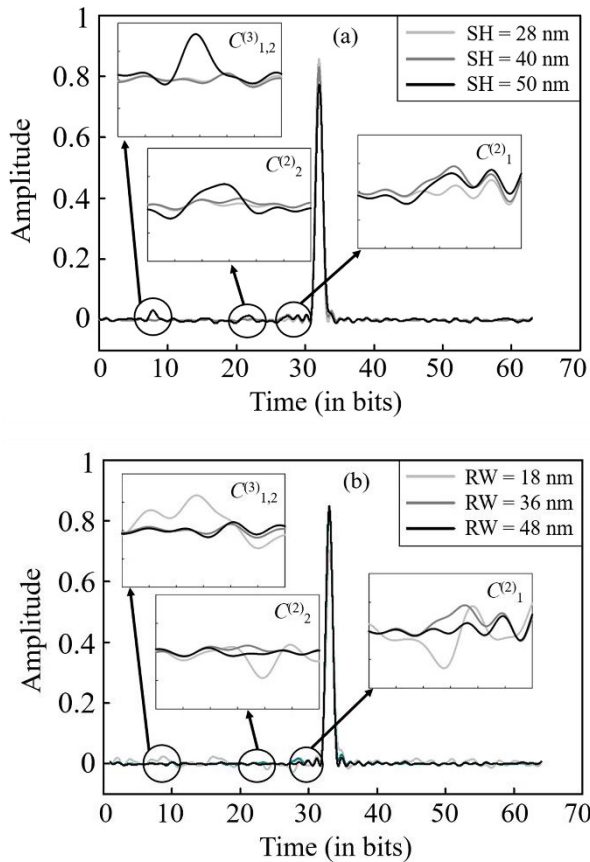


**FIGURE 3.** The dibit response of the readback signal generated by the CPP-GMR sensors at various lengths of (a) SH and (b) RW. The insets show the magnified image at each echo position.

As shown in Fig. 4, an asymmetry parameter of the readback signal was calculated showing that the readback signal became more asymmetric at shorter RW lengths and longer SH lengths. However, the asymmetry was slightly decreased when the SH was increased from 40 nm to 50 nm. The rationale of the reader sizing impact on the asymmetry can be explained as follows: since the free layer magnetization was aligned with its easy axis along the RW side, then an increase of RW typically yielded a longer easy-plane which results in the more stable magnetization precession. The reader with a longer RW can also have better stray field detection [33]. These matters yield the higher symmetrical readback waveform. On the other hand, lengthening the SH could cause higher asymmetry of the readback signal due to the highly fluctuated magnetization precession. However, a change in the SH at high values might have a small impact on asymmetry since the SH side has less affection on the stray field receiving capability than the RW side.

The noise occurring in the CPP-GMR readers was characterized through the integrated PSD of the playback response of the heads, as shown in Fig. 5. It was found that the PSD could be reduced either by shortening the SH length or increasing the length of RW. A change in SH length had a more influential impact on the PSD than that of the

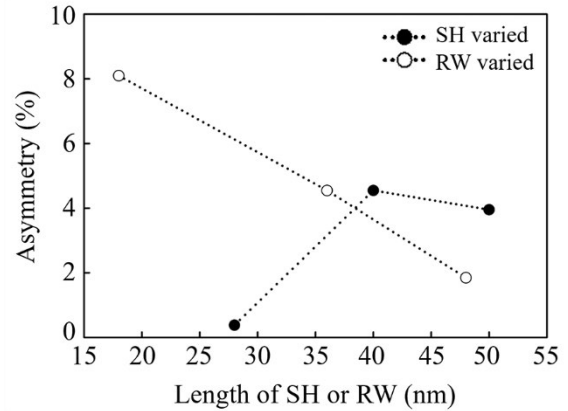


**FIGURE 4.** The asymmetry of the readback signal with different SH and RW.

RW length. Variations of SH at above the conventional value and that of RW below the conventional value caused a slight change to the PSD. However, the PSD was highly varied either by a change in SH below the conventional value or in RW above the conventional value. The rationale behind a reduction of PSD at shorter SH or longer RW lengths is due to the stronger shape anisotropy field at a higher easy/hard axes ratio. Therefore, the reader having short SH or long RW lengths could indicate a more stable magnetization precession with significantly smaller PSD intensity.

For further details of the PSD configuration, the frequency spectrum of the CPP-GMR response was characterized, as shown in Fig. 6. When the SH length was reduced from the conventional value (40 nm) to 28 cm, the resonance peak was shifted from 5 GHz to 5.5 GHz with a reduction of the integrated PSD. A very high PSD peak was clearly demonstrated at the SH length of 50 nm. When reducing the length of RW, the larger PSD peak appeared at higher frequencies. Meanwhile, the reader with longer RW produced a smaller integrated PSD, with a trivial variation of the resonance peak. From the analysis, an alternation of the physical dimensions of the CPP-GMR reader caused only a slight change in the spectral peak frequency.

The influence of bias current amplitude on the readback signal was also taken into account. Figure 7 shows the integrated PSD of the head response under the bias current densities of  $9.1 \times 10^6$  A/cm<sup>2</sup>,  $27.3 \times 10^7$  A/cm<sup>2</sup> and  $45.5 \times 10^7$  A/cm<sup>2</sup>, which are 1, 3 and 5 times of the conventional value, respectively. All bias current magnitudes were below the critical value for spin-torque induced instability. Similar to the previously evaluated conditions, the RW length was fixed while varying SH and vice versa. It was clearly seen that the PSD amplitude was extremely enhanced by increasing the bias current. The explanation of PSD enlargement is that the larger bias current magnitudes normally cause a stronger STT effect on the magnetization precession. Accordingly, the higher STT could highly induce the magnetization fluctuation, causing a larger PSD scale. When the bias current was increased, the change of PSD amplitude at different

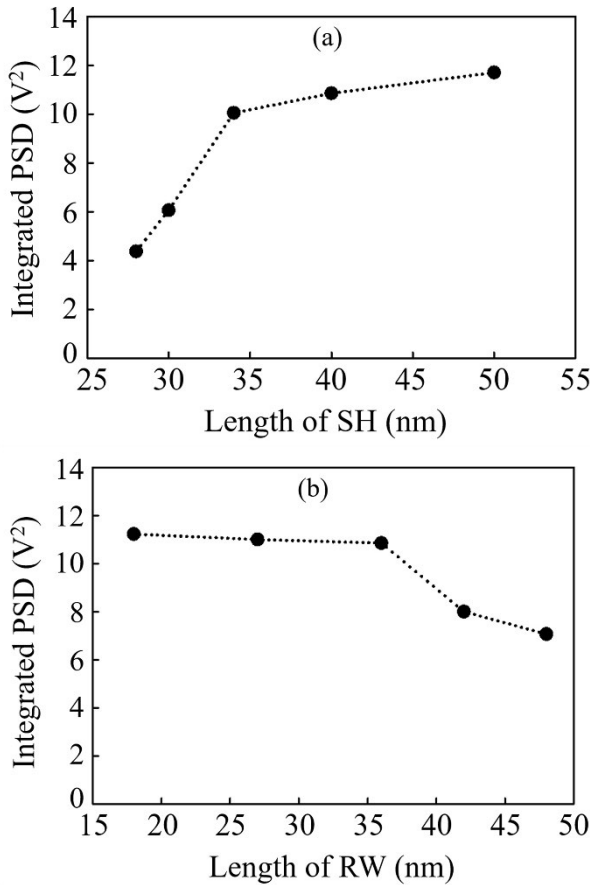


**FIGURE 5.** The integrated PSD of the CPP-GMR sensors response having different lengths of (a) SH and (b) RW.

reader dimensions was similar to that of the conventional bias current, confirming that the PSD behavior has the linearity property as a function of bias current.

From the above results, the appropriate physical dimensions of the CPP-GMR read sensors for AD of 1 Tb/in<sup>2</sup> was predicted based on the following discussions. Our analysis showed that either shortening the SH or increasing the RW can reduce the distortion as well as the instability of the head response, therefore both strategies should be performed as much as possible under the following conditions. In the read head design, the reader width is a crucial factor closely related to an increase in AD in which the bit size needs to be shrunk. Then, the RW should be firstly set before estimating the SH. At a particular track width, the maximum physical RW can be determined by the RW/track width ratio of 0.95 [37], beyond this value, the signal processing performance can drop significantly. Then, we predicted that the suitable RW for the CPP-GMR read sensors should be 48 nm in this particular circumstance. The reader having the RW of 48 nm also demonstrated the high symmetrical waveform. When estimating the appropriate SH length, it should be noted that the height of SH is strongly related to the stability of magnetization precession, which is typically dominated by the shape anisotropy field. As previously mentioned, the sensors are well-stabilized at a shorter SH due to a higher shape

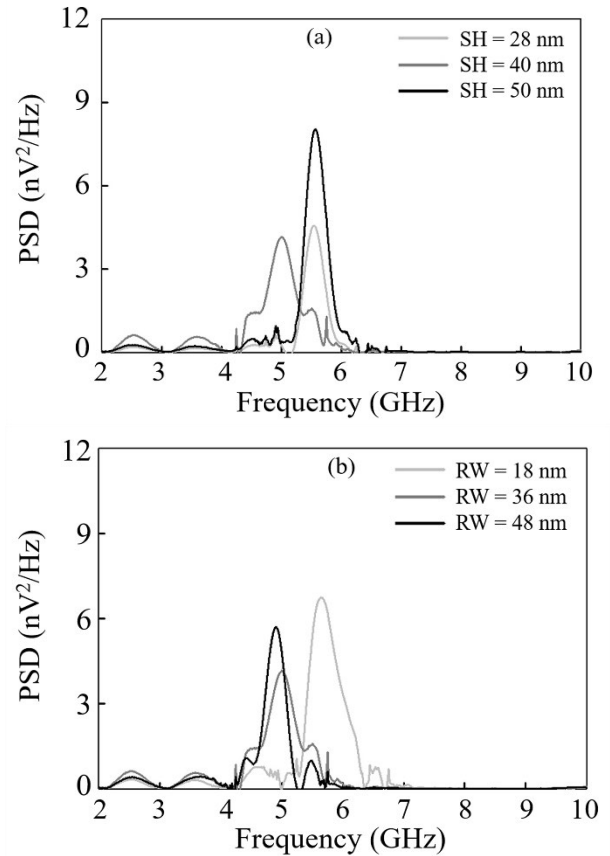


**FIGURE 6.** The spectral profile of the CPP-GMR response having different lengths of (a) SH and (b) RW.

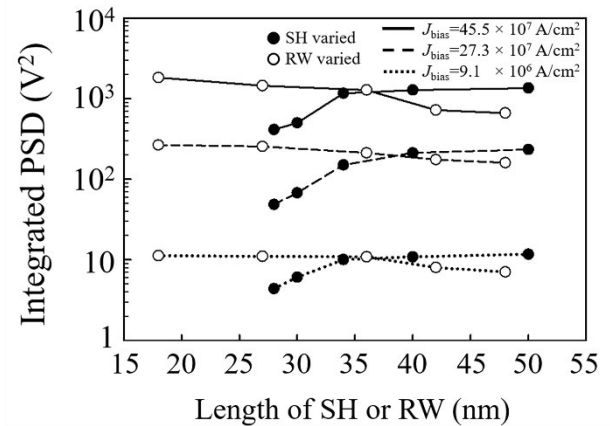


**FIGURE 7.** Influences of various current densities on the PSD of CPP-GMR read heads at various lengths of (a) SH and (b) RW.

anisotropy field. In contrast, the sensor utilization may be reduced in the case that the SH is shortened beyond the limitation. Nevertheless, the sensor utilization factor was neglected in this work since we assumed that the magnetization of the free layer is  $\pm 30^\circ$  tilted while operating in all cases. Another concerning factor related to the SH length is that a short SH improves the free layer stability and reduces the mag-noise, but tends to destabilize the reference layer.

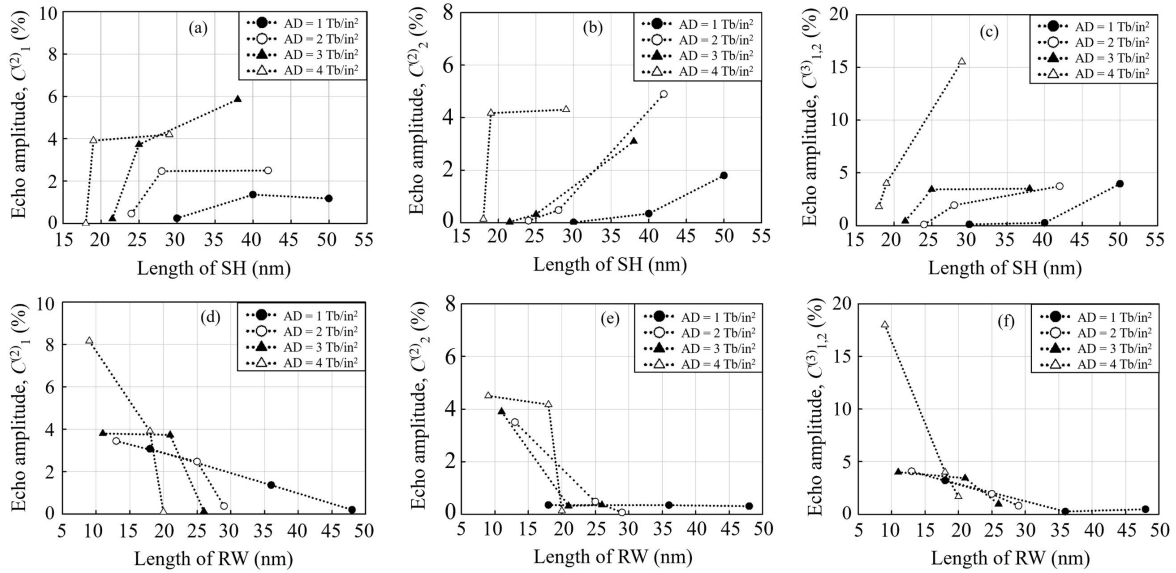


**FIGURE 8.** The echo amplitude of dibit response of the CPP-GMR read heads for AD of 1-4 Tb/in<sup>2</sup>. Figures. 8(a), 8(d) are C<sub>1</sub><sup>(2)</sup>, 8(b), 8(e) are C<sub>2</sub><sup>(2)</sup> and 8(c), 8(f) are C<sub>1,2</sub><sup>(3)</sup> of the reader having different lengths of SH and RW.

More than a decade ago, several studies suggested that the SH/RW ratio should be 1~1.1 to maintain stability between the free and the reference layers [2], [18], [20]. However, this limitation can be alleviated by using the extended reference layer, as widely proposed in many recent works [38]–[41]. Therefore, we predict that the optimal SH length should be set at the point at which the sensor utilization is still able to be maintained, which is 40 nm for this particular circumstance.

**B. OPTIMAL SIZING OF THE CPP-GMR READER FOR ADS UP TO 4 TB/in<sup>2</sup>**

In this sub-section, the optimal sizing of the CPP-GMR reader for ADs of 2-4 Tb/in<sup>2</sup> was predicted through the echo amplitude of the dibit response and the integrated PSD. The conventional dimension of the CPP-GMR read heads for ADs of 2, 3 and 4 Tb/in<sup>2</sup> was adopted from [18]. Similar to the procedure performed in sub-section 3.I, the possible range of SH and RW of the readers at each AD was varied and limited by the condition that the readers could be operated with ±30° tilt of free layer magnetization while receiving the H<sub>stray</sub>. It is noted that the length of RW was fixed while varying SH length and vice versa. The magnitude of H<sub>stray</sub> for each AD was calculated using a numerical calculation [30], and the compatible HB magnitude was calculated at each reader dimension for sensor stabilization. The simulation conditions of the readers for ADs of 1-4 Tb/in<sup>2</sup> are listed in Table 1.

The echo amplitude of dibit response of the CPP-GMR read heads at various ADs is shown in Fig 8. The echoes C<sub>1</sub><sup>(2)</sup>, C<sub>2</sub><sup>(2)</sup> and C<sub>1,2</sub><sup>(3)</sup> are displayed in figures 8(a)-(b), 8(c)-(d) and 8(e)-(f), respectively. The amplitude of echoes was normalized by its maximum scale and presented as a percentage. It was found that all echo amplitudes became larger at higher ADs. Also, all echoes increased either with increasing SH or decreasing RW length. At AD of 4 Tb/in<sup>2</sup>,

**TABLE 1.** The simulation conditions for the CPP-GMR readers at ADs of 1-4 Tb/in.

AD (Tb/in <sup>2</sup> )	1	2	3	4
TPI (kTPI)	500	707	866	1000
BPI (kBPI)	2000	2828	3464	4000
Reader gap (nm)	24.7	16	12.4	9.7

some echoes could be extremely enlarged due to the very small physical dimensions. The overall trend of echo amplitude was consistent with those of the reader for AD of 1 Tb/in<sup>2</sup>.

Figure 9 demonstrates the integrated PSD of the CPP-GMR readers for ADs of 1-4 Tb/in<sup>2</sup> at various SH and RW lengths. The results show a rapid enlargement of the PSD at higher ADs. This implies that the output response of the CPP-GMR read heads could be fluctuated increasingly at higher ADs due to the larger mag-noise. The rationale behind enhancement of PSD is given as follows: to achieve higher recording densities, both the bit size and reader dimensions need to be downsized. For the smaller sensors, it would be more difficult to control the magnetization precession stably, due to the limitation of the magnetic field amplitude applied for sensor stabilization. Therefore, the magnetization precession of the smaller sensors becomes increasingly unstable; meanwhile, the sensors are typically more sensitive to interference, i.e. the mag-noise. The results also corresponded to the fact that at higher ADs, where a higher sampling rate with a wider bandwidth is required, the noise power is expected to be increased. Another finding was that the variation of reader sizing indicates a more influential impact on the noise scale at higher recording densities, as can be seen from the PSD behavior. Similarly, to the PSD behavior of a 1 Tb/in<sup>2</sup> reader,

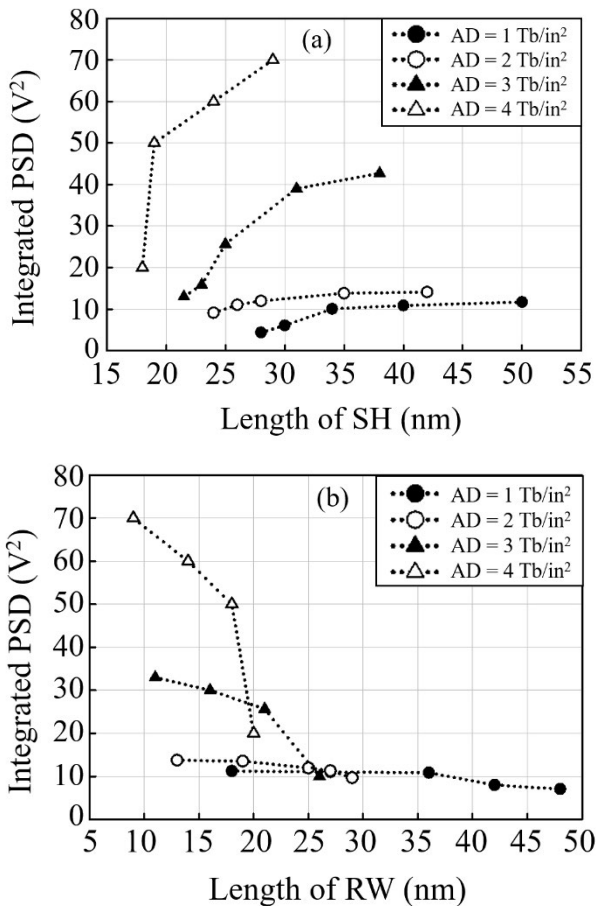


FIGURE 9. The integrated PSD of the CPP-GMR read heads for AD of 1–4 Tb/in<sup>2</sup> with varying (a) SH and (b) RW.

the PSD can be rapidly changed when shortening SH below the conventional value or increasing RW above the conventional value. Also, a variation of SH indicates a stronger impact on the PSD variation than that of RW. From our overall analysis, we predict that the optimal dimension (SH × RW) of the CPP-GMR read heads for ADs of 1, 2, 3 and 4 Tb/in<sup>2</sup> should be (40 × 48) nm, (28 × 29) nm, (25 × 26) nm and (19 × 20) nm, respectively. It should be noted that, at higher ADs, magnetization noise is another concerning factor that can be enlarged at smaller reader volume [42], [43]. The use of wider bandwidth at higher ADs may also increase reader noise power. Therefore, those factors need to be carefully handled and minimized. Findings in this work can be utilized for the design of the CPP-GMR sensors at ultrahigh area densities of magnetic recording technology.

#### IV. CONCLUSION

The optimal length of SH and RW of the CPP-GMR read heads for ADs of 1–4 Tb/in<sup>2</sup> was estimated through the performance indicators of the reader output including the readback signal, asymmetry parameter, dibit response and PSD profile. It was found that the reader having the shorter SH or longer RW length could produce a well-patterned readback waveform with smaller distortions, better resolution, and more

stable magnetization precession. The shape anisotropy field was the main influential factor dominating the distortion behavior. Also, the spectrum of the head response showed that a modification of reader dimension caused a slight change in the resonance peak. In addition, the linear increment of the PSD at higher bias current amplitudes was demonstrated. From the results, the optimal physical dimension (SH × RW) of the CPP-GMR reader for ADs of 1, 2, 3 and 4 Tb/in<sup>2</sup> was predicted to be (40 × 48) nm, (28 × 29) nm, (25 × 26) nm and (19 × 20) nm, respectively. The results can be utilized to design CPP-GMR sensors at ultrahigh magnetic recording densities.

#### ACKNOWLEDGMENT

Pirat Khunkitti would like to thank Dr. Tomoya Nakatani from the National Institute for Materials Science (NIMS), Japan, for his helpful discussion.

#### REFERENCES

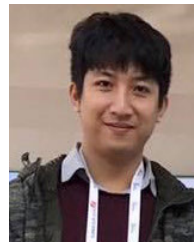
- [1] K. S. Chan, Y. Kanai, R. Itagaki, and S. Rahardja, “Optimization of the spin-torque oscillator response for microwave-assisted magnetic recording,” *IEEE Access*, vol. 7, pp. 140134–140141, 2019.
- [2] M. Takagishi, K. Yamada, H. Iwasaki, H. N. Fuke, and S. Hashimoto, “Magnetoresistance ratio and resistance area design of CPP-MR film for 2–5 Tb/in<sup>2</sup> read sensors,” *IEEE Trans. Magn.*, vol. 46, no. 6, pp. 2086–2089, Jun. 2010.
- [3] P. Khunkitti, A. Kruesubthaworn, A. Kaewrawang, and A. Siritatiwat, “Unstable playback response of CPP-GMR read head induced by electromagnetic interference: Structural dependence,” *IEEE Trans. Magn.*, vol. 55, no. 12, pp. 1–6, Dec. 2019.
- [4] K. Nagasaka, “CPP-GMR technology for magnetic read heads of future high-density recording systems,” *J. Magn. Magn. Mater.*, vol. 321, pp. 508–511, Mar. 2009.
- [5] M. Takagishi, K. Koi, M. Yoshikawa, T. Funayama, H. Iwasaki, and M. Sahashi, “The applicability of CPP-GMR heads for magnetic recording,” *IEEE Trans. Magn.*, vol. 38, no. 5, pp. 2277–2282, Sep. 2002.
- [6] Z. Diao, M. Chapline, Y. Zheng, C. Kaiser, and A. G. Roy, “Half-metal CPP GMR sensor for magnetic recording,” *J. Magn. Magn. Mater.*, vol. 356, pp. 73–81, Apr. 2014.
- [7] J. R. Childress, M. J. Carey, S. Maat, and N. Smith, “All-metal current-perpendicular-to-plane giant magnetoresistance sensors for narrow-track magnetic recording,” *IEEE Trans. Magn.*, vol. 44, no. 1, pp. 90–94, Jan. 2008.
- [8] J. R. Childress and R. E. Fontana, “Magnetic recording read head sensor technology,” *Comp. Rendus Phys.*, vol. 6, no. 9, pp. 997–1012, Nov. 2005.
- [9] E. E. Fullerton and J. R. Childress, “Spintronics, magnetoresistive heads, and the emergence of the digital world,” *Proc. IEEE*, vol. 104, no. 10, pp. 1787–1795, Oct. 2016.
- [10] N. Nakatani, S. Imai, M. A. Tanaka, T. Kubota, K. Takanashi, and K. Mibu, “Deposition temperature dependence of interface magnetism of Co<sub>2</sub>FeGe-Heusler-alloy/Ag films studied with <sup>57</sup>Fe Mössbauer spectroscopy,” *J. Magn. Magn. Mater.*, vol. 464, pp. 71–75, Oct. 2018.
- [11] T. Nakatani, Z. Gao, and K. Hono, “Read sensor technology for ultrahigh density magnetic recording,” *MRS Bull.*, vol. 43, no. 2, pp. 106–111, Feb. 2018.
- [12] T. M. Nakatani, N. Hase, H. S. Goripati, Y. K. Takahashi, T. Furubayashi, and K. Hono, “Co-based Heusler alloys for CPP-GMR spin-valves with large magnetoresistive outputs,” *IEEE Trans. Magn.*, vol. 48, no. 5, pp. 1751–1757, May 2012.
- [13] Z. Wen, T. Kubota, Y. Ina, and K. Takanashi, “Dual-spacer nanojunctions exhibiting large current-perpendicular-to-plane giant magnetoresistance for ultrahigh density magnetic recording,” *Appl. Phys. Lett.*, vol. 110, no. 10, Mar. 2017, Art. no. 102401.
- [14] Y. Du, T. Furubayashi, T. T. Sasaki, Y. Sakuraba, Y. K. Takahashi, and K. Hono, “Large magnetoresistance in current-perpendicular-to-plane pseudo spin-valves using Co<sub>2</sub>Fe(Ga<sub>0.5</sub>Ge<sub>0.5</sub>) Heusler alloy and AgZn spacer,” *Appl. Phys. Lett.*, vol. 107, no. 11, Sep. 2015, Art. no. 112405.



- [15] K. Goto, S. Liu, and Y. Du, "Magnetic and electrical properties of Heusler alloy Co<sub>2</sub>MnSi thin films grown on Ge(001) substrates via an Al<sub>2</sub>O<sub>3</sub> tunnel barrier," *Phys. Rev. Mater.*, vol. 4, Nov. 2020, Art. no. 114406.
- [16] T. Sato, S. Kokado, S. Kosaka, T. Ishikawa, T. Ogawa, and M. Tsunoda, "Large negative anisotropic magnetoresistance in Co<sub>2</sub>MnGa Heusler alloy epitaxial thin films," *Appl. Phys. Lett.*, vol. 113, no. 11, Sep. 2018, Art. no. 112407.
- [17] B. Pradines, L. Calmels, and R. Arras, "Robustness of the half-metallicity at the interfaces in Co<sub>2</sub>MnSi-based all-full-Heusler-alloy spintronic devices," *Phys. Rev. Appl.*, vol. 15, Mar. 2021, Art. no. 034009.
- [18] G. C. Han, J. J. Qiu, L. Wang, W. K. Yeo, and C. C. Wang, "Perspectives of read head technology for 10 Tb/in<sup>2</sup> recording," *IEEE Trans. Magn.*, vol. 46, no. 3, pp. 709–714, Mar. 2010.
- [19] J.-G. Zhu and X. Zhu, "Spin transfer induced noise in CPP read heads," *IEEE Trans. Magn.*, vol. 40, no. 1, pp. 182–188, Jan. 2004.
- [20] N. Smith, J. A. Katine, J. R. Childress, and M. J. Carey, "Thermal and spin-torque noise in CPP (TMR and/or GMR) read sensors," *IEEE Trans. Magn.*, vol. 42, no. 2, pp. 114–119, Feb. 2006.
- [21] P. Khunkitti, A. Kruesubthaworn, A. Kaewrawang, and A. Siritariwat, "Playback signal distortion in CPP-GMR read heads due to induced electromagnetic interference," *J. Magn. Magn. Mater.*, vol. 465, pp. 14–18, Nov. 2018.
- [22] A. Stankiewicz, T. Pipathanapoompran, K. Subramanian, and A. Kaewrawang, "Reader noise due to thermally driven asymmetric oscillations," *IEEE Trans. Magn.*, vol. 54, no. 11, pp. 1–5, Nov. 2018.
- [23] T. Pipathanapoompran, A. Stankiewicz, J. Wang, K. Subramanian, and A. Kaewrawang, "Magnetic reader testing for asymmetric oscillation noise," *J. Magn. Magn. Mater.*, vol. 514, Nov. 2020, Art. no. 167064.
- [24] T. Mewes, C. K. A. Mewes. (2012). *MATLAB Based Micromagnetics Code M3*. Accessed: Oct. 11, 2020. [Online]. Available: <http://magneticslab.ua.edu/micromagnetics-code.html/>
- [25] T. Nakatani, S. Li, Y. Sakuraba, T. Furubayashi, and K. Hono, "Advanced CPP-GMR spin-valve sensors for narrow reader applications," *IEEE Trans. Magn.*, vol. 54, no. 2, pp. 1–11, Feb. 2018.
- [26] D. Weller, A. Moser, L. Folks, M. E. Best, W. Lee, M. F. Toney, M. Schwickert, J.-U. Thiele, and M. F. Doerner, "High K<sub>u</sub> materials approach to 100 Gbits/in<sup>2</sup>," *IEEE Trans. Magn.*, vol. 36, no. 1, pp. 10–15, Jan. 2000.
- [27] W. Tipcharoen, A. Kaewrawang, and A. Siritariwat, "Design and micro-magnetic simulation of Fe/L1<sub>0</sub>-FePt/Fe trilayer for exchange coupled composite bit patterned media at ultrahigh areal density," *Adv. Mater. Sci. Eng.*, vol. 2015, Feb. 2015, Art. no. 504628.
- [28] K. Pituso, A. Kaewrawang, P. Buatong, A. Siritariwat, and A. Kruesubthaworn, "The temperature and electromagnetic field distributions of heat-assisted magnetic recording for bit-patterned media at ultrahigh areal density," *J. Appl. Phys.*, vol. 117, Jan. 2015, Art. no. 17C501.
- [29] F. J. MacWilliams and N. J. A. Sloane, "Pseudo-random sequences and arrays," *Proc. IEEE*, vol. 64, no. 12, pp. 1715–1729, Dec. 1976.
- [30] D. Litvinov, M. H. Kryder, and S. Khizroev, "Recording physics of perpendicular media: Hard layers," *J. Magn. Magn. Mater.*, vol. 241, pp. 453–465, Mar. 2002.
- [31] J. C. Slonczewski, "Current-driven excitation of magnetic multilayers," *J. Magn. Magn. Mater.*, vol. 159, nos. 1–2, pp. L1–L7, Jun. 1996.
- [32] P. Kovintavewat, I. Ozgunes, E. Kurtas, J. R. Barry, and S. W. McLaughlin, "Generalized partial-response targets for perpendicular recording with jitter noise," *IEEE Trans. Magn.*, vol. 38, no. 5, pp. 2340–2342, Sep. 2002.
- [33] P. A. A. van der Heijden, D. W. Karns, T. W. Clinton, S. J. Heinrich, S. Batra, D. C. Karns, T. A. Roscamp, E. D. Boerner, and W. R. Eppler, "The effect of media background on reading and writing in perpendicular recording," *J. Appl. Phys.*, vol. 91, pp. 8372–8374, May 2002.
- [34] D. Palmer, P. Ziperovich, R. Wood, and T. Howell, "Identification of non-linear write effects using pseudorandom sequences," *IEEE Trans. Magn.*, vol. 23, no. 5, pp. 2377–2379, Sep. 1987.
- [35] W. R. Eppler and I. Ozgunes, "Channel characterization methods using dipulse extraction," *IEEE Trans. Magn.*, vol. 42, no. 2, pp. 176–181, Feb. 2006.
- [36] R. D. McMichael and M. D. Stiles, "Magnetic normal modes of nanoelements," *J. Appl. Phys.*, vol. 97, no. 10, 2005, Art. no. 10J901.
- [37] K. S. Chan, A. James, S. Shafiee, S. Rahardja, J. Shen, K. Sivakumar, and B. J. Belzer, "User areal density optimization for conventional and 2-D detectors/decoders," *IEEE Trans. Magn.*, vol. 54, no. 2, pp. 1–12, Feb. 2018.
- [38] M. M. Pinarbasi, "Magnetic head having CPP sensor with improved stabilization of the magnetization of the pinned magnetic layer," U.S. Patent 9 007 727, Apr. 14, 2015.
- [39] Q. Le, S. H. Liao, G. Liu, K. Ju, and Y. Zheng, "Magnetic sensor having an extended pinned layer with stitched antiferromagnetic pinning layer," U.S. Patent 9 202 482, Dec. 1, 2015.
- [40] Y. Ahn, D. P. Druist, Z. Gao, Y. Hong, and Y. Huang, "Magnetic read sensor with independently extended pinned layer and seed layer," U.S. Patent 9 053 721, Jun. 9, 2015.
- [41] P. M. Braganca, M. J. Carey, J. R. Childress, and Y. S. Choi, "Magnetic recording head with CPP-GMR spin-valve sensor and extended pinned layer," U.S. Patent 9 130 055, Sep. 8, 2015.
- [42] Y. Wang, M. F. Erden, and R. H. Victora, "Novel system design for readback at 10 terabits per square inch user areal density," *IEEE Magn. Lett.*, vol. 3, Art. no. 4500304.
- [43] Y. Wang, M. F. Erden, and R. H. Victora, "Novel system design for readback at 10 terabits per square inch user areal density," *IEEE Magn. Lett.*, vol. 3, no. 3, Mar. 2012, Art. no. 3100606.



**PIRAT KHUNKITTI** (Member, IEEE) received the B.E. degree (Hons.) and the Ph.D. degree in electrical engineering from Khon Kaen University, Thailand, in 2012 and 2016, respectively. Currently, he is working as an Professor at KKU-Seagate Cooperation Research Laboratory, Department of Electrical Engineering, Faculty of Engineering, Khon Kaen University. His research interests include magnetic recording heads, spintronics, electrostatic discharge, electromagnetic interference, permanent magnet machine, permanent magnet generator, and power systems. He has received many scholarships from Thailand Research Fund and the National Research Council of Thailand. He is an Assistant Editor of the *Engineering and Applied Science Research*.



**KOTCHAKORN PITUSO** received the B.E. and M.E. degrees in electrical engineering from Khon Kaen University, Khon Kaen, Thailand, in 2011 and 2014, respectively, and the Ph.D. degree in information and system engineering from King Mongkut's Institute of Technology Ladkrabang (KMITL), in 2019. He is currently a Senior Engineer with the Electrical Development Engineering Department, Seagate Technology (Thailand) Ltd.



**NUTTAPON CHAIDUANGSRI** received the B.S. and M.S. degrees in electrical engineering from Khon Kaen University, Khon Kaen, Thailand, in 2012 and 2014, respectively. He is currently pursuing the Ph.D. degree in electrical engineering with King Mongkut's Institute of Technology Ladkrabang, Bangkok, Thailand. Since 2014, he has been a Research and Development Engineer with Seagate Technology (Thailand) Ltd. His research interests include the magnetic recording and signal processing.



**APIRAT SIRITARIWAT** received the B.E. degree in electrical engineering from Khon Kaen University, Thailand, in 1992, and the Ph.D. degree from The University of Manchester, U.K., in 1999. After completing his B.E. degree, he worked at the industry for a few years, after that he joined the Department of Electrical Engineering, Khon Kaen University, in 1994. Currently, he is working with KKU-Seagate Cooperation Research Laboratory, Department of Electrical Engineering, Faculty of

Engineering, Khon Kaen University. He has done many researches with more than 100 publications in ESD/EOS and EMI area. Also, he is one of the pioneer researchers in the area of magnetism in Thailand and has done a lot of works with HDD industries.

...